

# Smoothing seismicity techniques applied to seismic source characterization and probabilistic seismic hazard analysis in Brazil

Marlon Pirchiner<sup>1,2</sup> and Marcelo Assumpção<sup>1</sup>

---

Corresponding author: Marlon Pirchiner, Department of Geophysics, IAG, USP, São Paulo, Brazil. (marlon.pirchiner@iag.usp.br)

<sup>1</sup>Department of Geophysics, Institute of Astronomy, Geophysics and Atmospherical Sciences (IAG), University of São Paulo (USP), São Paulo, Brazil.

<sup>2</sup>Applied Math School (EMAp), Getúlio Vargas Foundation (FGV), Rio de Janeiro, Brazil.

Intraplate seismicity is a hard problem to solve in tectonics, mainly during the lack of observed seismicity in many areas where seismic hazard assessment are also difficult and the methods applied are often close correlated to the geometries defined by the experts with valuable criteria.

Three smoothing seismicity techniques are reviewed and their application to the Brazilian seismicity and a seismic hazard assessment are discussed.

All these smoothing methods are based on a Kernel Density Estimation (KDE). The main difference between them is the bandwidth selection process.

The method of *Frankel* [1995] uses a *fixed* bandwidth in space. *Woo* [1996] suggests a bandwidth as function of the *magnitude*. *Helmstetter and Werner* [2012] propose a *locally-adaptive* kernel bandwidths in space and time, chosen for each event.

This last one was proposed initially to take care of the background seismicity rate in the context of long-term earthquake forecast which time-independence assumption able us to use this recurrence rate to define a grid of seismic point sources as the input source model to compute the hazard.

The results shown that all methods clearly define some known seismic regions and could be used in the Brazilian seismicity. All methods improve the spatial resolution of the GSHAP model, the only previously available for the region.

All the hazard computations was performed on OpenQuake [*Pagani et al.*, 2014] open source software also from GEM Foundation.

## 1. Introduction

### 1.1. Intraplate seismicity

COMENTAR CAPITULO DO LIVRO

### 1.2. Previous studies in Brazil

Despite some studies of seismicity rates and attempts at defining the main seismic zones [*Berrocal et al.*, 1984, 1996; *Assumpção et al.*, 2014], Brazil has no seismic hazard map at national scale.

The Brazilian seismic hazard building code [*ABNT*, 2006] was based on the GSHAP [*Giardini et al.*, 1999] results for South America [*Tanner and Shepherd*, 1997; *Shedlock and Tanner*, 1999], which is the last published model for the whole region. However, some significant seismic areas (Porto dos Gaúchos [*Barros et al.*, 2009]), are not represented in the GSHAP-based building codes.

A significant number of earthquakes has been recorded in the last decades [*BSB*, 2014] allowing a better empirical and updated definition of the seismicity and hazard levels.

### 1.3. Smoothed seismicity

Although the standard *Cornell* [1968] and *McGuire* [1976] methodology often used to assess seismic hazard is using expert opinions to pre-defined seismic zones, the goal of this paper is to review a few smoothing seismicity methods based on KDE which results in a grid of smoothed seismicity without define any seismic zone polygon.

The KDE (or smoothed) seismicity grid allow to define a grid of seismic point sources. The seismic rate (*a*-value) associated to each source is defined by the smoothed seismicity methods, but the other parameters, like *b*-values, minimum and maximum magnitudes, rupture and depth distributions, must be assigned in other ways.

To perform the KDE, both its shape and bandwidth needs to be defined. Most kernels are Gaussian or power-laws or one of their variants. The main distinction between the methods described here is the bandwidth selection process.

*Frankel* [1995] smoothing method applies a Gaussian *Nadaraya* [1964]-*Watson* [1964] smoothing technique with a *fixed* smoothing-distance bandwidth to estimate the seismicity rate smoothing the 2D histogram counting. This version of the algorithm is already implemented on the Hazard Modeller's Toolkit (HMTK) [*Weatherill et al.*, 2012; *Weatherill*, 2014]. There is also a simple variant of Frankel's method discussed by *Zechar and Jordan* [2010] which sum the contribution of each earthquake kernel on given cell. *Woo* [1996] proposes a *magnitude-dependent* kernel bandwidth based on the nearest neighbor mean distance in magnitude bins. *Helmstetter and Werner* [2012] proposes a *locally-adaptive* bandwidth, based on kernel estimations for the background seismicity rate in long-term forecasts on both space and time dimensions.

Using the background seismic rate computed to the forecast and assuming time-independence of that, the same assumption of PSHA, it is possible, preserving their differences [*Marzocchi and Zechar*, 2011], to use these forecasted seismicity values on seismic sources characterization [*Weatherill and Pagani*, 2014].

#### 1.4. Hazard computation

To perform the hazard computation, the OpenQuake suite [*Pagani et al.*, 2014] was chosen. The modelling tool was the HMTK also open available by Global Earthquake Model (GEM) scientific board. The Frankel method was already implemented on the toolkit and the other two was implemented in the context of this paper and they are free available on a public repository.

The earthquake catalog data comes from the Brazilian seismological research authorities.

### **1.5. Specific purposes**

The specific purposes of this paper are: (i) review 3 distincts smoothing/zoneless methods to describe spatially the seismicity rate, (ii) update the seismic hazard studies at national scale by proposing a new hazard model, (iii) use the GEM-OpenQuake tools to perform hazard calculation and (iv) add and share with the community two more new smoothing methods into the HMTK.

To aim this, the Brazilian seismicity data is presented including some overview plots. Next the method's theory is presented follow by the specific decisions and optimizations performed on each method modelling. And last, the results, conclusions and further considerations are discussed.

## **2. Brazilian seismicity data**

Data on intraplate seismicity in Brazil is currently the Brazilian Seismic Bulletin maintained mainly by the Seismological Center of the University of São Paulo [BSB, 2014]. This catalog is a joint compilation from different sources.

### **2.1. Hypocenters**

For events up to 1981, the catalog corresponds to *Berrocal et al.* [1984] which is a comprehensive compilation of historic and instrumental data with participation of Universidade de São Paulo (USP), Universidade de Brasilia (UnB), Universidade Federal do Rio Grande do Norte (UFRN), Observatório Nacional (ON) and Instituto de Pesquisas Tecnológicas do Estado de São Paulo (IPT). From 1982 to 1995 the information comes from the annual bulletins published by Revista Brasileira de Geofísica. Since 1995, the Bulletin is maintained mainly by USP under the same cooperation network in addition

to Universidade Estadual Paulista (UNESP). Earlier versions of this catalog were used to compose the well-known *CERESIS* [1985, 1995] catalogs.

Today the catalog is distributed in two ways. One, which could be called *raw*, contains all compiled information, such as: events outside the country which were felt in Brazil, errors in previous versions and also non-seismic events (known quarry blasts, sonic boom, etc). The other way could be called *clean*, where all non-seismic and low quality events were removed. This last one was used in this paper and the total number of entries is [CALCULAR O NUMERO DE EVENTOS NO CATALOGO].

This catalog only cover crustal events. Andean subduction earthquakes deeper than 50km in the Brazil-Peru border was discarded. The epicenters of the catalog are shown in figure 1.

## 2.2. Magnitudes

Most magnitudes were computed as *mb* type or the equivalent *mR* [Assumpção, 1983] regional magnitude. For historical events magnitudes were estimated from macroseismic data (felt area and maximum intensity) [Berrocal *et al.*, 1984]. Since most GMPE are based on *M<sub>W</sub>* moment scale magnitude, in this present study, we converted all *mb* magnitudes to *M<sub>W</sub>* values following the guidelines on table 1. REFERENCIA PARA STEPHANE/ASSUMPCAO WORK IN PROGRESS. (Johnston)

## 2.3. Catalog checking

Figure 2 shows the distribution of depths, day of the week and origin hour following *Gulia et al.* [2012]. Most events have no depth determination and the well determined depths (from *pP* phases or local networks) are mostly less than 10km.

Figures 2b and 2c show an almost uniform distribution of day of the week, and a slight trend to record earthquakes during the night. This could suggest some influence of daily noise level.

The annual number of earthquakes since 1900 (figure 3) shows a steady increase since 1960 and two peaks in 1986 and 1998 derived from two large seismic sequences: João Câmara [Takeya *et al.*, 1989] and Porto dos Gaúchos [Barros *et al.*, 2009]. The increasing number of records after 1960 is due to the operation of global, regional and local stations.

#### 2.4. Declustering procedures

To preserve the Poissonian assumption about the independence of the events, several declustering algorithms were tried and the results as shown in figure 4a. The window-method [Gardner and Knopoff, 1974] was tested with three different windows: Gardner and Knopoff [1974], Uhrhammer [1986] and Grüenthal [van Stiphout *et al.*, 2012]. In addition the algorithm (AFTERAN) proposed by Musson [1999] was also tested using Grüenthal distance window.

In the case of Brazilian catalog the methods did not present large differences at the final number of earthquakes (fig. 4a) and the Gardner-Knopoff/Uhrhammer combination was chosen to maximize the number of events.

The map of figure 4b locates all clusters in the catalog. It is an *a-priori* evidence of regions in Brazil where long earthquake series tend to occur more frequently.

#### 2.5. Frequency-magnitude distribution

Figure 6 presents the catalog Magnitude Frequency Distribution (MFD). A general  $b = 1$  fit is also plotted, and the completeness magnitude on the incremental distribution is about 3.0.

## 2.6. Catalog completeness

The completeness of Brazilian seismicity data has evident time and space dependence. Brazil just recently was installed its permanent seismic network [Pirchner *et al.*, 2011]. The number and quality of stations increased over time. The population density, previously concentrated along the coast increased in other regions changing the historical detectability.

There are many methodologies to assessment of the temporal and spatial completeness [Stepp, 1972; Mignan and Wöessner, 2012; Ogata and Katsura, 1993; Wiemer and Wyss, 2000; Cao and Gao, 2002; Stucchi *et al.*, 2004; Woessner, 2005; Mignan *et al.*, 2011; Mignan, 2012; Vorobieva *et al.*, 2013; Mignan *et al.*, 2013; Nasir *et al.*, 2013; Mignan and Chouliaras, 2014], or explaining how to compute the real Probability of Detecting an Earthquake (PDE) from the waveforms [Schorlemmer and Woessner, 2008], but the time and the effort to proceed this exhaustive study of the completeness magnitude, despite its relevance, was not intended to be done on the scope of this paper.

The waveforms from the earliest years was not in digital form. The histories of most regional (temporary) stations are not easy available. In addition, the low number of earthquakes in the catalog also difficults some high resolution statistical methods. All of this hinders the direct application of most that methodologies.

For this reason, the spatial completeness was not considered and the temporal completeness parameters for the whole country was defined by an easy cumulative rate criteria using historical information about the network evolution and the *Stepp* [1972] plot (fig. 5a). TALK ABOUT BRASILIA STATION???

Figure 5b shows the magnitude time distribution in a scatter plot as the cumulative number of events which is important to perform the temporal course of earthquake frequency (TCEF) [Nasir *et al.*, 2013]. The linear behavior of cumulative rate on the

recent years, gives an idea about the constant record trend. Figure 5b also show three (from many) possible completeness tables to allow quick check their distinctions. We chosen the “simplest” one.

## IMPROVE THIS DECISION EXPLANATION

### 3. Smoothing methods

Three smoothing methods are now briefly explained.

#### 3.1. Frankel: fixed bandwidth

*Frankel* [1995] smoothing seismicity proposal consisted originally in using a “correlation distance”  $d_F$  as the *fixed* kernel bandwidth and applying the Nadaraya-Watson [Nadaraya, 1964; Watson, 1964] estimator to smooth a 2D seismicity histogram using a Gaussian kernel:

$$\tilde{n}_j = \frac{\sum_i n_i e^{-\left(\frac{d_{ij}}{d_F}\right)^2}}{\sum_i e^{-\left(\frac{d_{ij}}{d_F}\right)^2}}, \quad (1)$$

where  $\tilde{n}_j$  is the smoothed seismicity (number of earthquakes with magnitude  $m$  above the minimum magnitude  $M_d$  in the catalog) on cell  $j$ .  $n_i$  is the earthquake counting in each other cell  $i$  and  $d_{ij}$  is distance between grid cells  $i$  and  $j$ .

#### 3.2. Woo: magnitude-dependent bandwidth

*Woo* [1996] suggested to evaluate the contribution of each earthquake  $i$ , located at  $\mathbf{r}_i$ , to the seismicity rate  $R$  (number of earthquakes per year and unity area) on the cell centered in  $\mathbf{r}$ , depending on the magnitude  $m$ :

$$R(\mathbf{r}, m) = \sum_{i=1}^N \frac{K(\mathbf{r} - \mathbf{r}_i, m)}{T(\mathbf{r}_i)}, \quad (2)$$

where  $N$  is the number of earthquakes  $i$  in the magnitude bin  $m \pm dm$ , and  $T(\mathbf{r}_i)$  is the completeness time of magnitude  $m$  observed on  $\mathbf{r}_i$ .

Any kernel could be applied on that definition. I used used the *Kagan and Knopoff* [1980] kernel for infinite spatial domain as described by *Woo* [1996]:

$$K_{KK}(\mathbf{r}, m | a_W) = \frac{a_W - 1}{\pi h(m)^2} \left[ 1 + \frac{\mathbf{r}^2}{h(m)^2} \right]^{-a_W}, \quad (3)$$

where  $a_W$  is fractal dimension factor, generally about 1.5 and 2 [*Vere-Jones*, 1992].

VERIFICAR SE É O CASO DE APRESENTAR OUTRAS FORMAS DE KERNEL.  
DAR PREFERENCIAS AOS REALMENTE UTILIZADOS.

To compute the magnitude-dependent bandwidth function  $h(m)$ , *Woo* [1996] suggested the follow relation

$$h(m | a_0, a_1) = a_0 e^{a_1 m}, \quad (4)$$

where  $a_0$  and  $a_1$  are computed by the regression of the mean nearest distance  $h$  from each magnitude bin  $m \pm dm$ , as illustrated on figure 7.

Just to compare, in figure 7 it is shown the functions computed by *Beauval* [2003] for Norway and Spain. The angular coefficient ( $a_1$ ) is in the same range of the others but the general mean distance between events into the same magnitude bin is higher than other countries. It is in some way expected. Brazil is quite large than mentioned countries.

### 3.3. Helmstetter and Werner: locally-adaptive space and time bandwidths

Even work on a forecast perspective, the background seismicity rate for a long-term time-independent forecast could be used to characterize a diffused seismicity under the common assumption that this background seismic rate is invariant over time.

*Helmstetter and Werner* [2012] proposes a seismicity model space and time dependent using kernels for space and time independently:

$$R(\mathbf{r}, t) = \sum_{i=1}^N \frac{1}{{h_i}^2} K_t \left( \frac{t - t_i}{h_i} \right) K_r \left( \frac{\|\mathbf{r} - \mathbf{r}_i\|}{d_i} \right), \quad (5)$$

where  $R(\mathbf{r}, t)$  is the seismic rate located  $\mathbf{r}$  distant from the earthquake occurred on the instant  $t$ ,  $K_t$  is the time domain kernel function, where  $t_i$  is the time location of earthquake  $i$  and  $h_i$  is the temporal bandwidth for earthquake  $i$ ,  $K_r$  is the space domain kernel function, where  $\mathbf{r}_i$  is the spatial location of earthquake  $i$  and  $d_i$  is the spatial bandwidth for earthquake  $i$ .

As they are interested in forecast, just past time  $t_i < t$  need to be considered. Also the observation completeness is taken in account by a set of weights  $w$  in this follow way:

$$R(\mathbf{r}, t) = R_{min} + \sum_{t_i < t} \frac{2w(\mathbf{r}_i, t_i)}{h_i d_i^2} K_t\left(\frac{t - t_i}{h_i}\right) K_r\left(\frac{\|\mathbf{r} - \mathbf{r}_i\|}{d_i}\right), \quad (6)$$

where  $R_{min}$  is the minimum seismic rate, positive, allowing earthquakes to occur where their never occurred yet.

The weights  $w(\mathbf{r}_i, t_i)$ , computed for each earthquake  $i$ , are the Gutenberg-Richter  $a$ -value projection. This is the expression used to compute it:

$$w(\mathbf{r}, t) = 10^{b(\mathbf{r}, t)[M_c(\mathbf{r}, t) - M_d]}, \quad (7)$$

where  $w$  is the weight factor computed on location  $\mathbf{r}$  on instant  $t$ ,  $b(\mathbf{r}, t)$  is the space and time dependent b-value,  $M_c(\mathbf{r}, t)$  is the completeness magnitude on location  $\mathbf{r}$  and  $t$ ,  $M_d$  is the minimum magnitude value on the catalogue.

These weights increase the seismicity contribution from earthquakes occurred where and when the completeness magnitude  $M_c$  was greater than minimum catalog magnitude  $M_d$ . They also could easily take into account the space and time completeness and  $b$ -value fluctuations.

### 3.3.1. Local bandwidth computation

The method implemented to compute the space and time bandwidths for each earthquake was the Coupled-Nearest-Neighbor (CNN) [Helmstetter and Werner, 2012] ex-

pressed as:

$$h_i, d_i = \arg \min_{\substack{h_i \geq h_k \\ d_i \geq d_k}} [s(h_i, d_i | k_{cnn}, a_{cnn}) := h_i + a_{cnn}d_i], \quad (8)$$

where  $k_{cnn}$  is the  $k^{th}$  nearest neighbor,  $a_{cnn}$  is a space-time coupling factor,  $d_k$  is the  $\max \{d_j\}, j = 1, \dots, k_{cnn}$  and  $h_k$  is the  $\max \{h_j\}, j = 1, \dots, k_{cnn}$ .

The bandwidths are defined locally by this simple optimization process. It could be small on high earthquake density regions and higher where earthquakes are rarely or regions with information lack.

### 3.3.2. Stationary seismic rate

After compute the model parameters it is completely defined, and the time-independent or stationary seismic rate  $\bar{R}$  on each location  $\mathbf{r}_0$  can be computed on the way proposed by *Helmstetter and Werner* [2012] taking the median value for some location  $\mathbf{r}_0$  over all considered time window:

$$\bar{R}(\mathbf{r}_0) = \text{Median}[R(\mathbf{r}_0, t)]. \quad (9)$$

The median should avoid the seismicity rate fluctuations derived by fore and aftershocks and consequently the decluster procedures. This is one of the most important achievement of this methodology.

### 3.3.3. Maximum likelihood optimization

The model is completely defined by  $k_{cnn}$ ,  $a_{cnn}$  and  $R_{min}$ . To optimize these parameters the catalog is divided in two parts: one for *learning* about the parameters and other to test them. The *testing* catalog will able us to check the model prediction performance derived from its chosen parameters. The best model parameters will maximize the prediction model capacity likely the target catalog.

If the earthquake occurrence could be modeled by a Poisson process with rate  $N_p$ , then the probability to observe exactly  $n$  events on the considered time frame is

$$p(N_p, n) = \frac{N_p^n e^{-N_p}}{n!}. \quad (10)$$

Then, over all cells, the log-likelihood, to be maximized, between model prediction (from the learning catalog) and the observed earthquakes (on the testing catalog) is written as

$$L = \sum_{i_x=1}^{N_x} \sum_{i_y=1}^{N_y} \log p [N_p(i_x, i_y), n(i_x, i_y)] \quad (11)$$

where  $N_p(i_x, i_y)$  is the predicted seismic rate on cell  $(i_x, i_y)$  and  $n(i_x, i_y)$  is the number of target earthquakes observed on cell  $(i_x, i_y)$ .

The model parameters  $R_{min}$ ,  $a_{cnn}$  and  $k_{cnn}$  should be optimized by the maximization of log-likelihood  $L$ .

## 4. Results

### 4.1. Simulations

#### 4.1.1. Simulation 1

## 5. Discussion

## Appendix A: Appendix Title

**Acknowledgments.** The author thanks specially to all IAG-USP seismological team. It is also grateful to Stéphane Drouet and Vincent Guigues for all helpful discussions.

## References

- ABNT, A. (2006), NBR 15421: Design of seismic resistant structures - procedures.
- Assumpção, M. (1983), A regional magnitude scale for brazil, *Bulletin of the Seismological Society of America*, 73(1), 237–246.
- Assumpção, M., J. Ferreira, L. Barros, H. Bezerra, G. S. França, J. R. Barbosa, E. Menezes, L. C. Ribotta, M. Pirchiner, A. do Nascimento, and J. C. Dourado (2014), Intraplate seismicity in Brazil, in *Intraplate Earthquakes*, pp. 50–71, Cambridge University Press.
- Barros, L. V., M. Assumpção, R. Quintero, and D. Caixeta (2009), The intraplate porto dos gaúchos seismic zone in the amazon craton — brazil, *Tectonophysics*, 469(1-4), 37–47, doi:10.1016/j.tecto.2009.01.006.
- Beauval, C. (2003), Analyse des incertitudes dans une estimation probabiliste de l'aléa sismique, exemple de la france, Ph.D. thesis, Université Joseph-Fourier-Grenoble I.
- Berrocal, J., U. de São Paulo. Instituto Astronômico e Geofísico, and B. C. N. de Energia Nuclear (1984), *Sismicidade do Brasil*, Instituto Astronômico e Geofísico, Universidade de São Paulo.
- Berrocal, J., C. Fernandes, A. Bassini, and J. R. Barbosa (1996), Earthquake hazard assessment in southeastern brazil, *Geofísica Internacional*, 35(3), 257–272.
- BSB (2014), Boletim Sísmico Brasileiro (BSB) version 2014.11. Institute of Astronomy, Geophysics and Atmospheric Sciences, University of São Paulo, IAG-USP.
- Cao, A., and S. S. Gao (2002), Temporal variation of seismic b-values beneath northeastern japan island arc, *Geophysical Research Letters*, 29(9), 48–1–48–3, doi: 10.1029/2001GL013775.
- CERESIS (1995), Catalogue for south america and the caribbean prepared in the framework of gshap, *Tech. rep.*, Centro Regional de Sismología para América del Sur.

CERESIS, S. T. A., Bonny L. Askew (1985), Catalog of earthquakes for south america,

*Tech. rep.*, CERESIS (Centro Regional de Sismología para América del Sur). Earthquake mitigation program in the Andean Region (SISRA project).

Cornell, C. A. (1968), Engineering seismic risk analysis, *Bulletin of the Seismological Society of America*, 58, 1583–1606.

Frankel, A. (1995), Mapping seismic hazard in the central and eastern united states, *Seismological Research Letters*, 66(4), 8–21.

Gardner, J. K., and L. Knopoff (1974), Is the sequence of earthquakes in southern california, with aftershocks removed, poissonian?, *Bulletin of the Seismological Society of America*, 64(5), 1363 – 1367.

Giardini, D., G. Grünthal, K. M. Shedlock, and P. Zhang (1999), The GSHAP global seismic hazard map, *Annali di Geofisica*, 42(6), 1225–1230.

Gulia, L., S. Wiemer, and M. Wyss (2012), Catalog artifacts and quality control, *Community Online Resource for Statistical Seismicity Analysis*, doi:10.5078/corssa-93722864.

Helmstetter, A., and M. J. Werner (2012), Adaptive spatiotemporal smoothing of seismicity for long-term earthquake forecasts in california, *Bulletin of the Seismological Society of America*, 102(6), 2518–2529.

Kagan, Y. Y., and L. Knopoff (1980), Spatial distribution of earthquakes: the two point correlation function, *Geophys. J. R. Astr. Soc.*, 62.

Marzocchi, W., and J. D. Zechar (2011), Earthquake forecasting and earthquake prediction: different approaches for obtaining the best model, *Seismological Research Letters*, 82(3), 442–448.

McGuire, K. K. (1976), FORTRAN computer program for seismic risk analysis, *Open-File report 76-67*, United States Department of the Interior, Geological Survey, 102

pages.

Mignan, A. (2012), Functional shape of the earthquake frequency-magnitude distribution and completeness magnitude, *Journal of Geophysical Research*, 117(B8), doi: 10.1029/2012JB009347.

Mignan, A., and G. Chouliaras (2014), Fifty years of seismic network performance in greece (1964–2013): Spatiotemporal evolution of the completeness magnitude, *Seismological Research Letters*, 85(3), 657–667, doi:10.1785/0220130209.

Mignan, A., and J. Wöessner (2012), Corssa - theme IV - estimating the magnitude of completeness for earthquake catalogs, *Tech. Rep.* doi: 10.5078/corssa-00180805, Community Online Resource for Statistical Seismicity Analysis.

Mignan, A., M. J. Werner, S. Wiemer, C.-C. Chen, and Y.-M. Wu (2011), Bayesian estimation of the spatially varying completeness magnitude of earthquake catalogs, *Bulletin of the Seismological Society of America*, 101(3), 1371–1385, doi: 10.1785/0120100223.

Mignan, A., C. Jiang, J. D. Zechar, S. Wiemer, Z. Wu, and Z. Huang (2013), Completeness of the mainland china earthquake catalog and implications for the setup of the china earthquake forecast testing center, *Bulletin of the Seismological Society of America*, 103(2A), 845–859, doi:10.1785/0120120052.

Musson, R. M. W. (1999), Probabilistic seismic hazard maps for the north balkan region, *Annali di Geofisica*, 42(2), 1109 – 1124.

Nadaraya, E. A. (1964), On estimating regression, *Theory of Probability & Its Applications*, 9(1), 141–142, doi:10.1137/1109020.

Nasir, A., W. Lenhardt, E. Hintersberger, and K. Decker (2013), Assessing the completeness of historical and instrumental earthquake data in austria and the surrounding areas, *Austrian Journal of Earth Sciences*, 106(1), 90–102.

Ogata, Y., and K. Katsura (1993), Analysis of temporal and spatial heterogeneity of magnitude frequency distribution inferred from earthquake catalogues, *Geophysical Journal International*, 113(3), 727–738, doi:10.1111/j.1365-246X.1993.tb04663.x.

Pagani, M., D. Monelli, G. Weatherill, L. Danciu, H. Crowley, V. Silva, P. Henshaw, L. Butler, M. Nastasi, L. Panzeri, M. Simionato, and D. Vigano (2014), OpenQuake engine: An open hazard (and risk) software for the global earthquake model, *Seismological Research Letters*, 85(3), 692–702, doi:10.1785/0220130087.

Pirchner, M., B. Collaço, J. Calhau, M. Assumpção, and J. C. Dourado (2011), The BRAzilian seismographic integrated systems (BRASIS): infrastructure and data management, *Annals of Geophysics*, (1), doi:10.4401/ag-4865.

Schorlemmer, D., and J. Woessner (2008), Probability of detecting an earthquake, *Bulletin of the Seismological Society of America*, 98(5), 2103 – 2117.

Shedlock, K. M., and J. G. Tanner (1999), Seismic hazard map of the western hemisphere, *Annals of Geophysics*, 42(6).

Stepp, J. C. (1972), Analysis of completeness of the earthquake sample in the Puget Sound area and its effects on statistical estimates of earthquake hazard, in *International Conference on Microzonation for Safer Construction Research and Application*, vol. 2, pp. 897–909, University of Seattle.

Stucchi, M., P. Albini, M. Mirto, and A. Rebez (2004), Assessing the completeness of italian historical earthquake data, *Annals of Geophysics*, 47(2-3).

Takeya, M., J. Ferreira, R. Pearce, M. Assumpção, J. Costa, and C. Sophia (1989), The 1986–1988 intraplate earthquake sequence near João Câmara, northeast Brazil: evolution of seismicity, *Tectonophysics*, 167(2-4), 117–131, doi:10.1016/0040-1951(89)90062-0.

Tanner, J. G., and J. B. Shepherd (1997), Seismic hazard in latin america and caribe,

*Tech. rep.*, PAIGH, Pan-American Institute of Geography and History.

Uhrhammer, R. (1986), Characteristics of northern and central california seismicity,

*Earthquake Notes*, 57(1), 21.

van Stiphout, T., J. Zhuang, and D. Marsan (2012), Theme V: Models and techniques for analysing seismicity, *Tech. rep.*, Community Online Resource for Statistical Seismicity Analysis.

Vere-Jones, D. (1992), Statistical methods for the description and display of earthquake catalogs, *Statistics in the Environmental and Earth Sciences*.

Vorobieva, I., C. Narteau, P. Shebalin, F. Beauducel, A. Nercessian, V. Clouard, and M.-P. Bouin (2013), Multiscale mapping of completeness magnitude of earthquake catalogs, *Bulletin of the Seismological Society of America*, 103(4), 2188–2202, doi: 10.1785/0120120132.

Watson, G. S. (1964), Smooth regression analysis, *Sankhya: The Indian Journal of Statistics, Series A (1961-2002)*, 26(4), pp. 359–372.

Weatherill, G. (2014), Hazard modeller's toolkit - user guide, *Tech. rep.*, Global Earthquake Model (GEM).

Weatherill, G., and M. Pagani (2014), From smoothed seismicity forecasts to probabilistic seismic hazard: insights and challenges from a global perspective, in *2nd European Conference on Earthquake Engineering and Seismology*, ECEES.

Weatherill, G. A., M. Pagani, and D. Monelli (2012), The hazard component of the GEM modeller's toolkit: A framework for the preparation and analysis of probabilistic seismic hazard (PSHA) input tools, in *Proceedings of the 15th World Conference on Earthquake Engineering, Lisbon, Portugal, paper*.

Wiemer, S., and M. Wyss (2000), Minimum magnitude of completeness in earthquake catalogs: Examples from alaska, the western united states, and japan, *Bulletin of the Seismological Society of America*, 90(4), 859–869, doi:10.1785/0119990114.

Woessner, J. (2005), Assessing the quality of earthquake catalogues: Estimating the magnitude of completeness and its uncertainty, *Bulletin of the Seismological Society of America*, 95(2), 684–698, doi:10.1785/0120040007.

Woo, G. (1996), Kernel estimation methods for seismic hazard area source modeling, *Bulletin of the Seismological Society of America*, 86(2), 353–362.

Zechar, J. D., and T. H. Jordan (2010), Simple smoothed seismicity earthquake forecasts for italy, *Annals of Geophysics*, 53(3), 99–105.

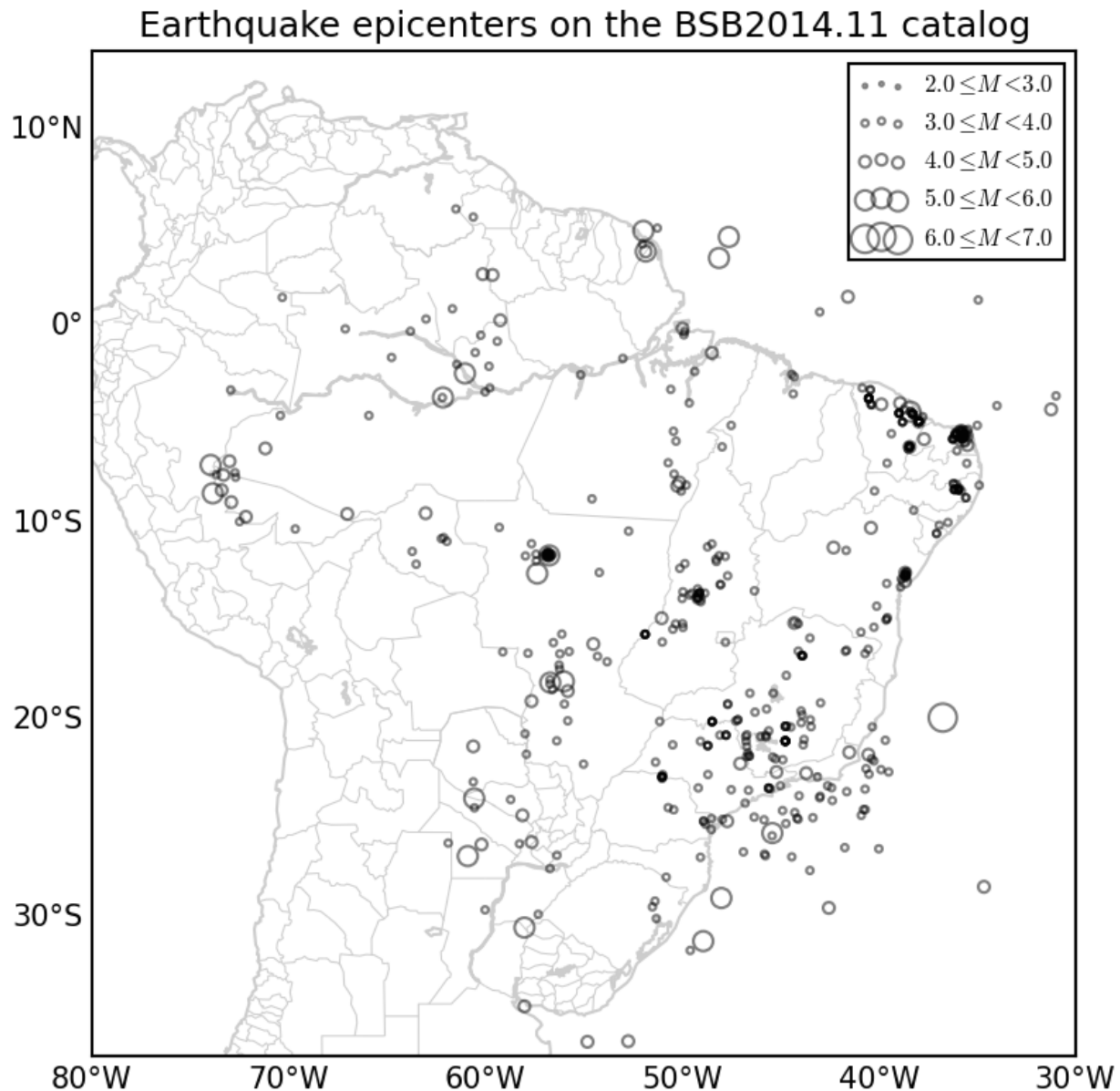


**Figure 1.** Brazilian seismicity from 1767 to 2014. Source: [BSB, 2014].

**Table 1.** BSB 2014.11  $M_W$  proxies *ad-hoc* guidelines.

magnitude source	rule	uncertainty
$mb$ or $mR$	$M_W(m) = 1.121m - 0.76$	0.3
Felt area $A_f$	$M_W(A_f) = 0.81 + 0.639 \log(A_f) + 0.00084\sqrt{A_f}$	0.4
Maximum intensity $I_0$	$mb(I_0) = 1.21 + 0.45I_0$ then $M_W(m)$	0.6
$mb$ and $A_f$	$M_W(m, A_f) = 0.7M_W(m) + 0.3M_W(A_f)$	0.33

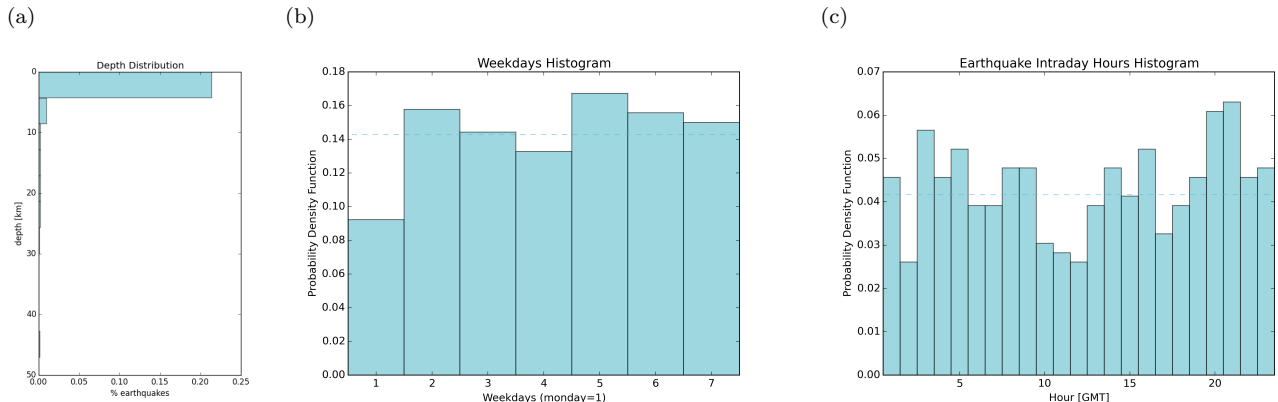


**Figure 2.** Catalogue overview. The histogram (a) shows the depth distribution. The histograms (b) and (c) represent the distributions of weekday and hour which earthquakes occur respectively. Dashed lines represent the mean value.

**Table 2.** Temporal completeness. For each magnitude interval, the completeness was computed

by the *Stepp* [1972] method.

magnitude	year (Stepp)
3.0	1970
4.0	1959
4.5	1951
6.0	1933

**Table 3.** Temporal completeness. For each magnitude interval, the completeness comes from

*Assumpção et al.* [2014] converted to  $M_W$  from  $m_b$  following table 1.

magnitude	year (Assumpção)
3.1	1980
4.3	1968
4.8	1962
6.0	1940

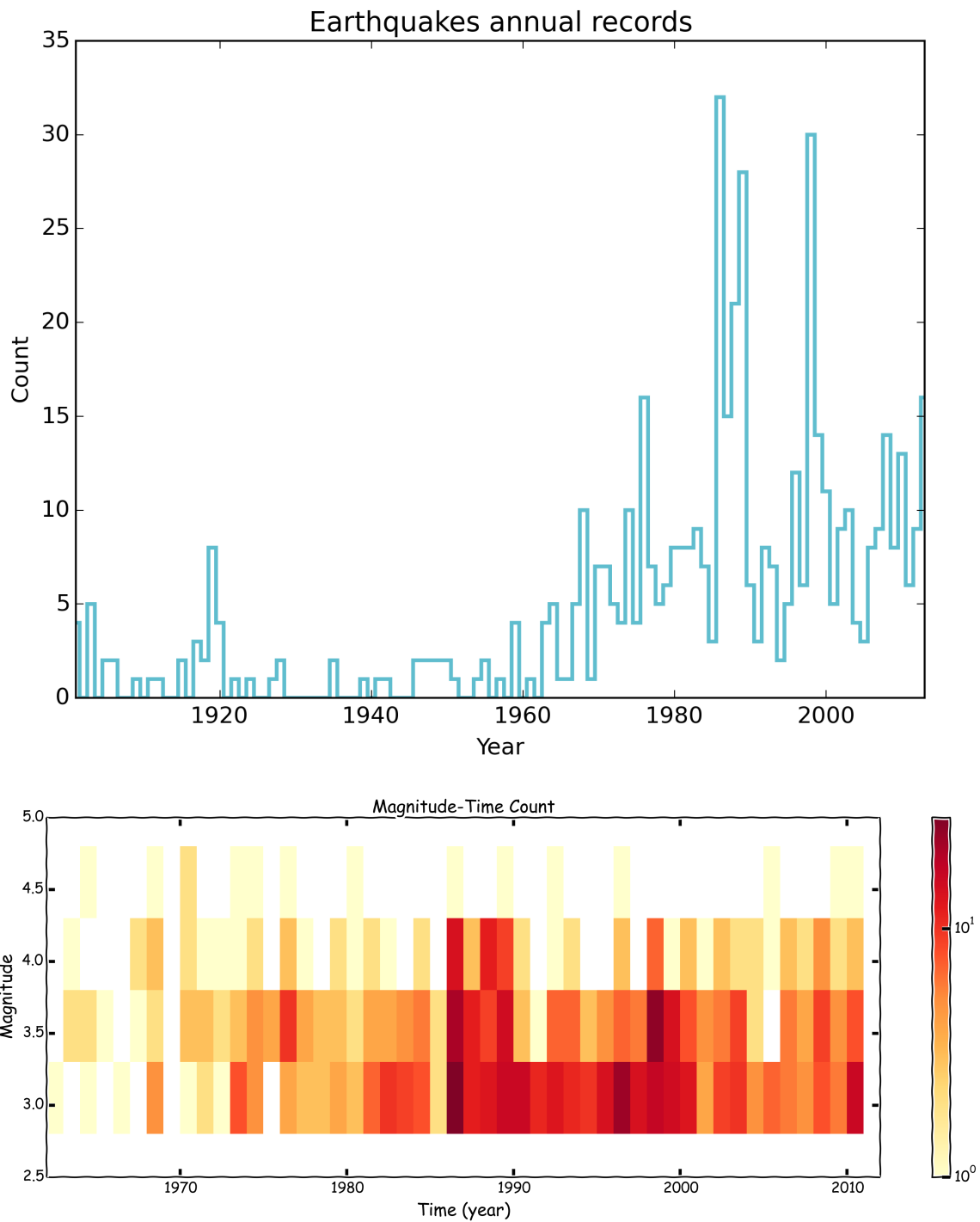
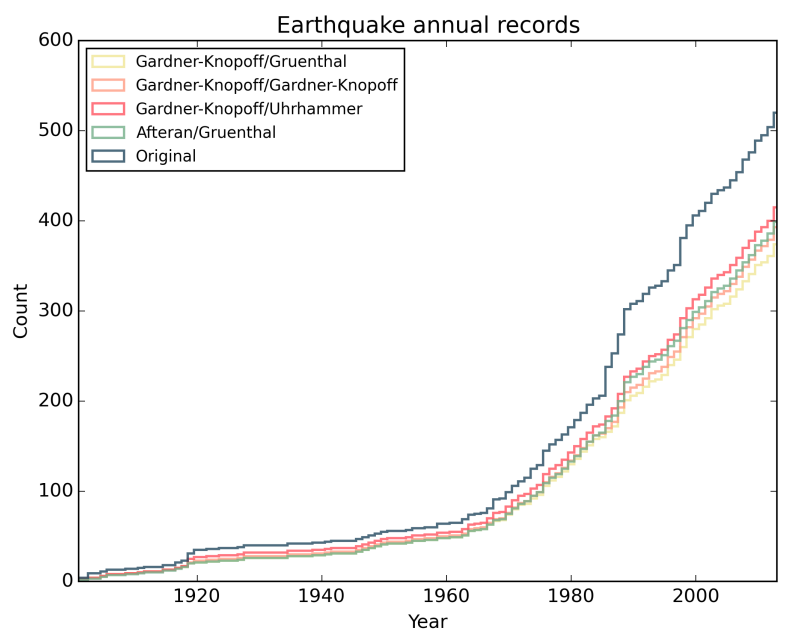
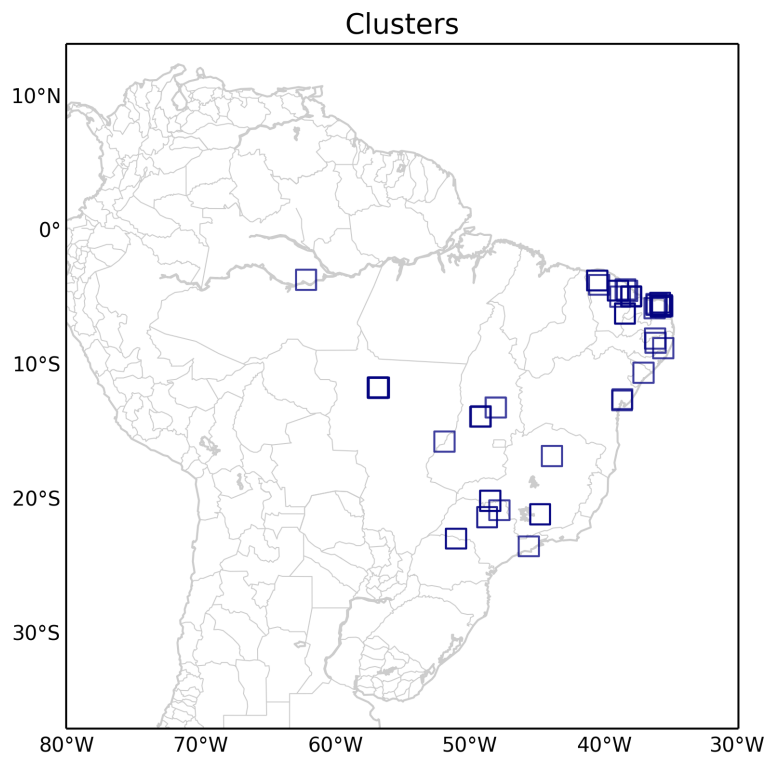


**Figure 3.** Earthquakes by year (a) and discriminated by magnitude (b).



(a)



(b)

**Figure 4.** Decluster evaluation (a) using distinct algorithms and windows. There is no significant differences between final results. The map (b) of clusters from selected method shows places where earthquake sequences tends to occur more frequently.

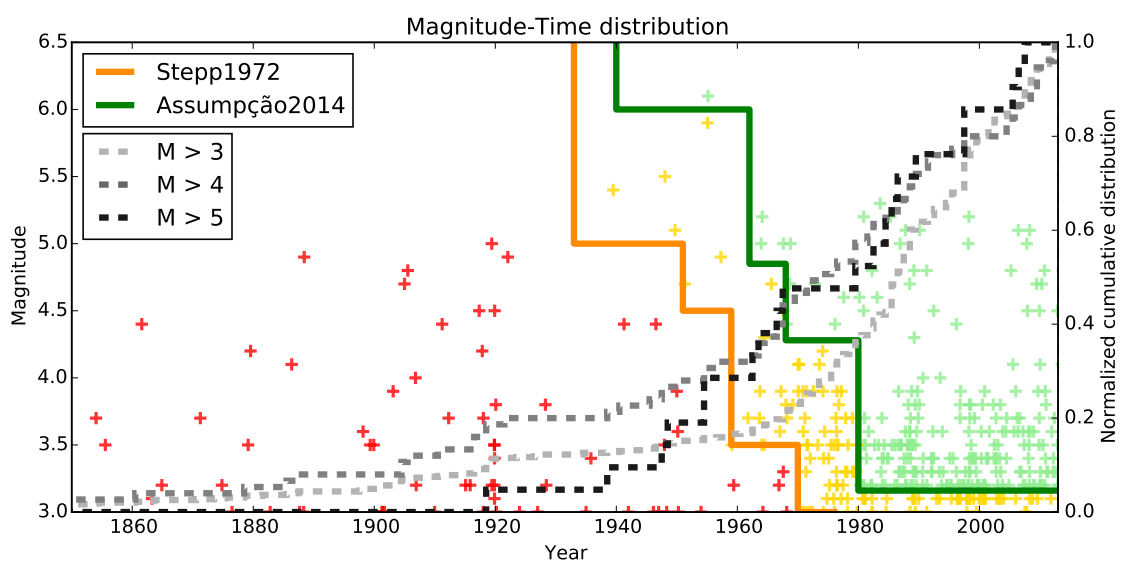
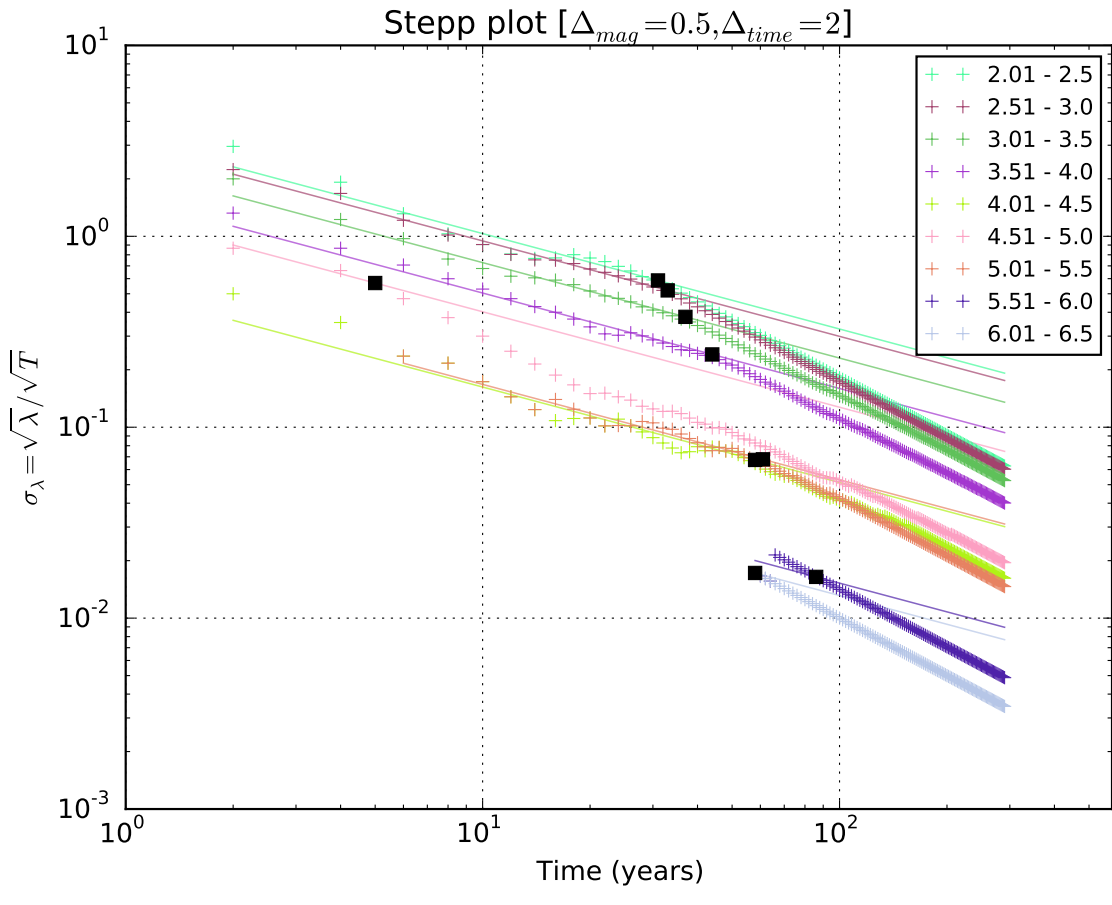


**Figure 5.** Completeness evaluation. The Stepp plot (a) was made using  $\Delta_{mag} = 0.5$  and  $\Delta_{time} = 2$  as magnitude and time bins. The magnitude-time scatter plot (b) shows in addition, three different temporal completeness models and some cumulative rates to better perform a visual analysis.

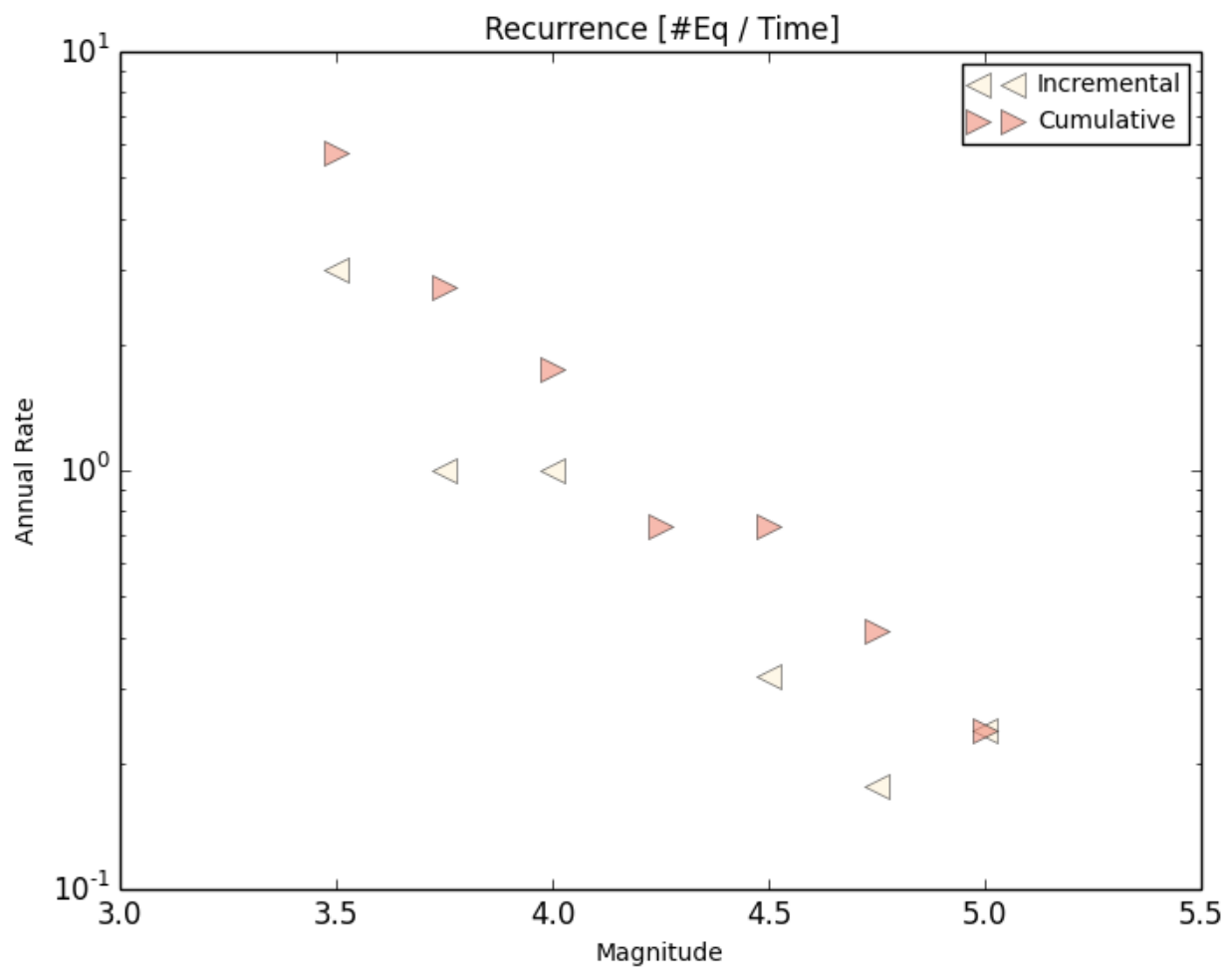


**Figure 6.** Annual earthquake recurrence.

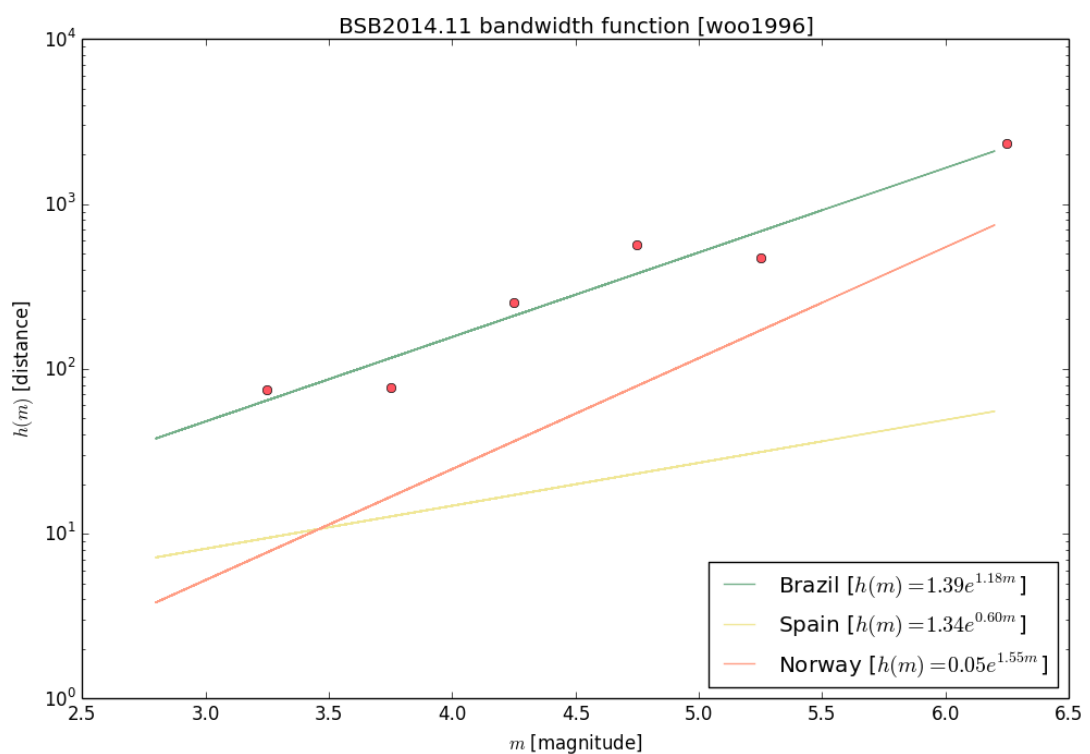


**Figure 7.** Magnitude dependence bandwidth.

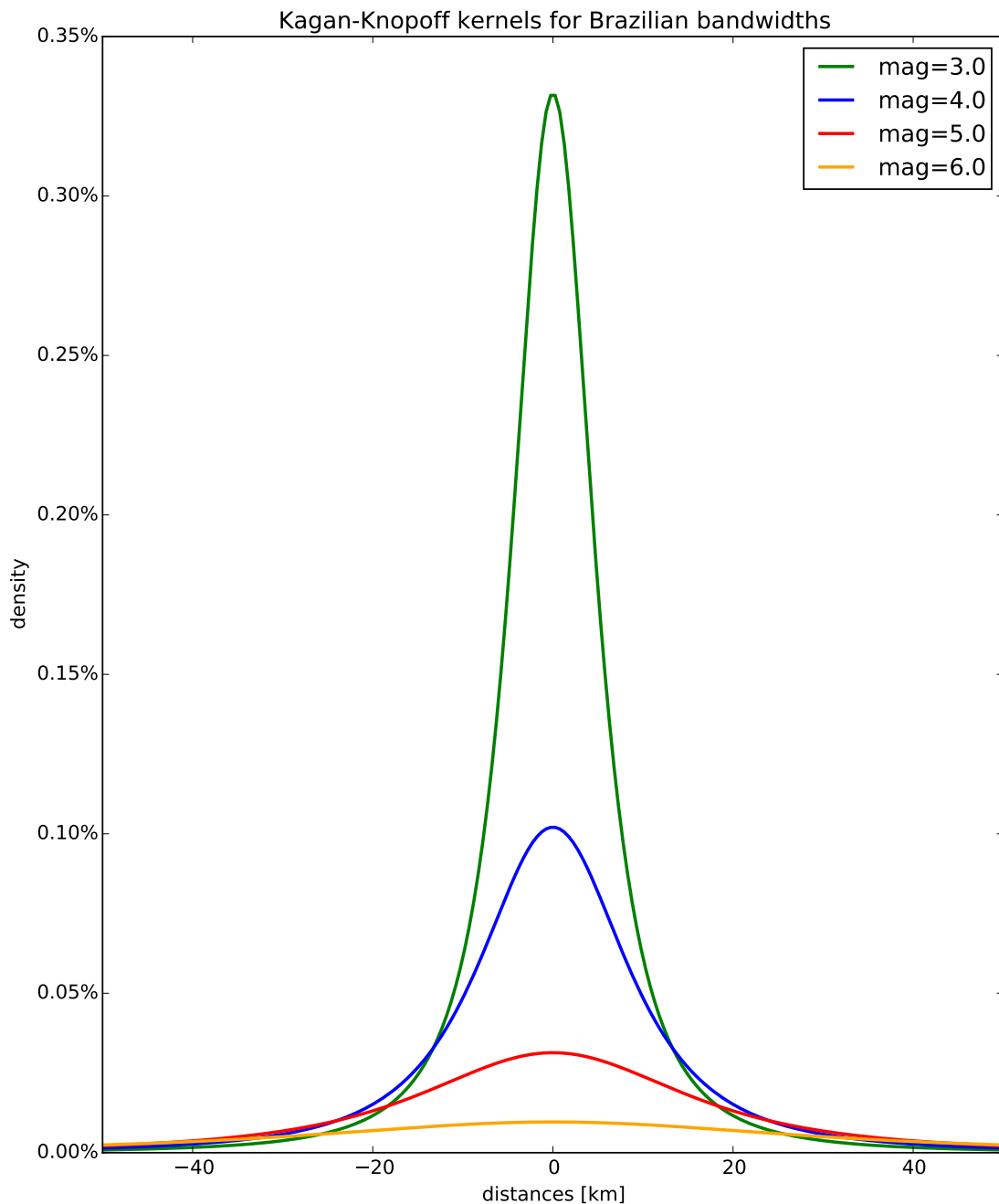


**Figure 8.** *Kagan and Knopoff* [1980] kernel shapes for some magnitude values.

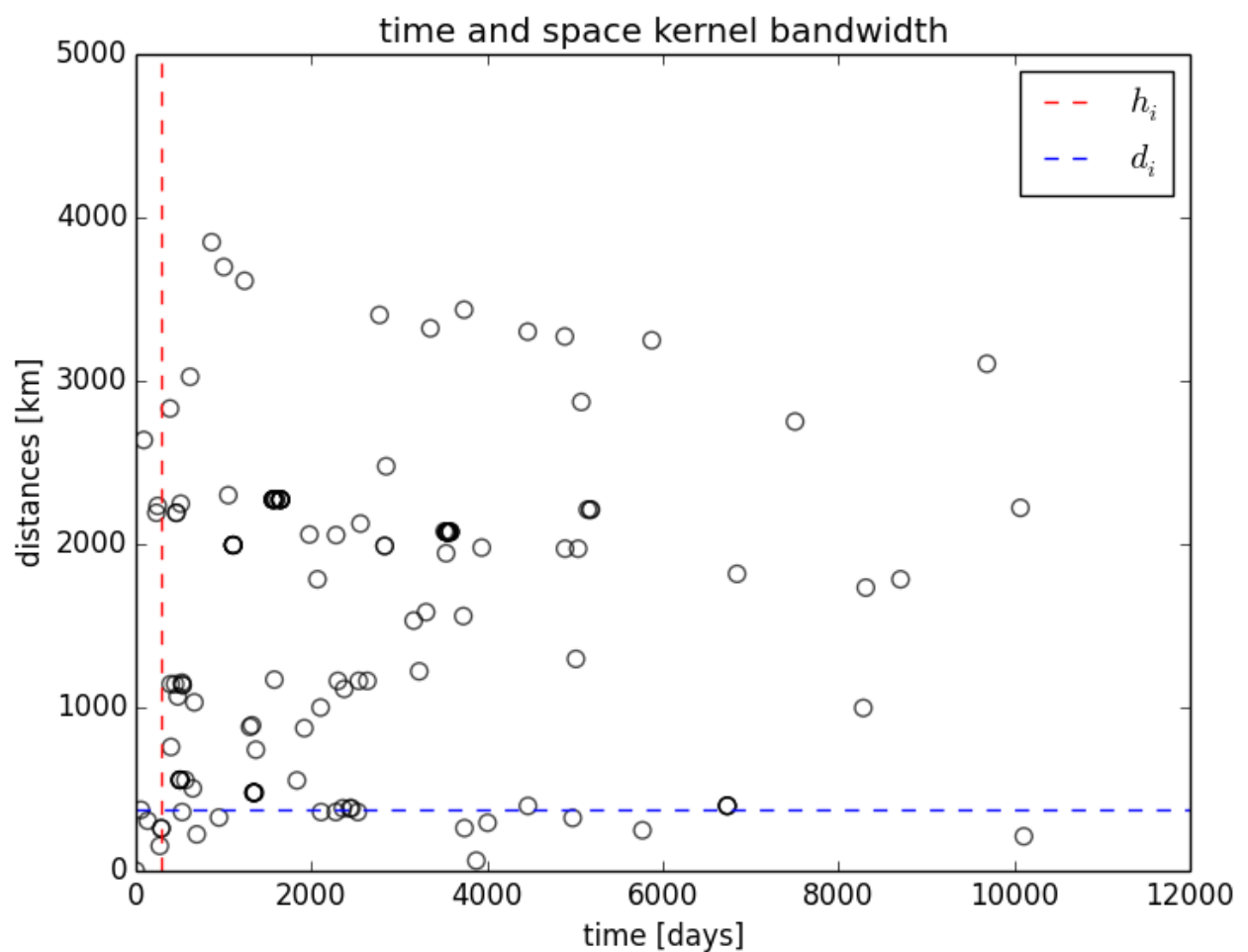
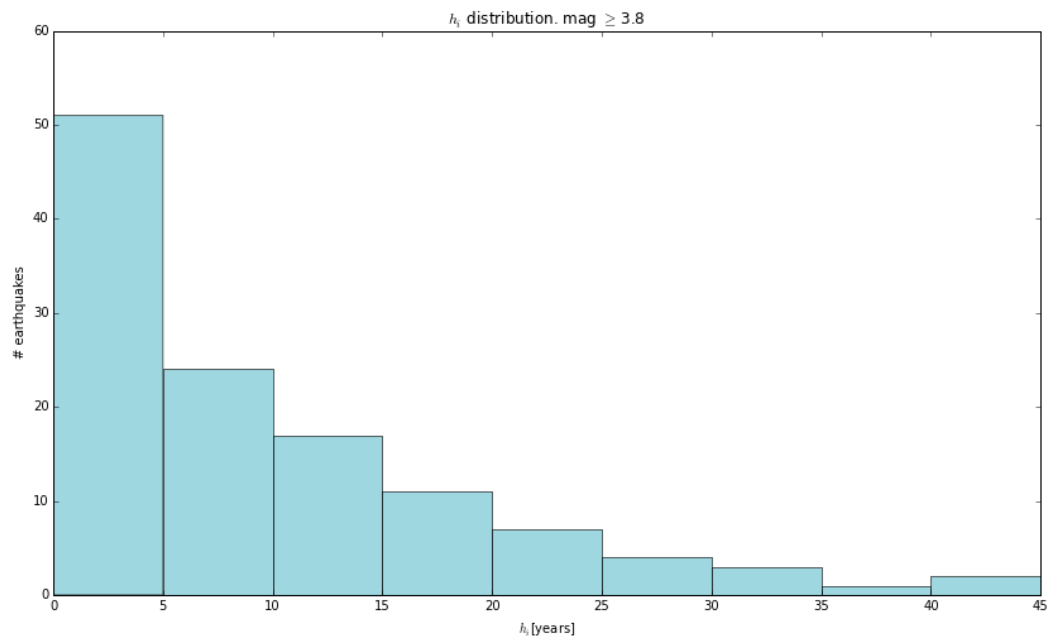
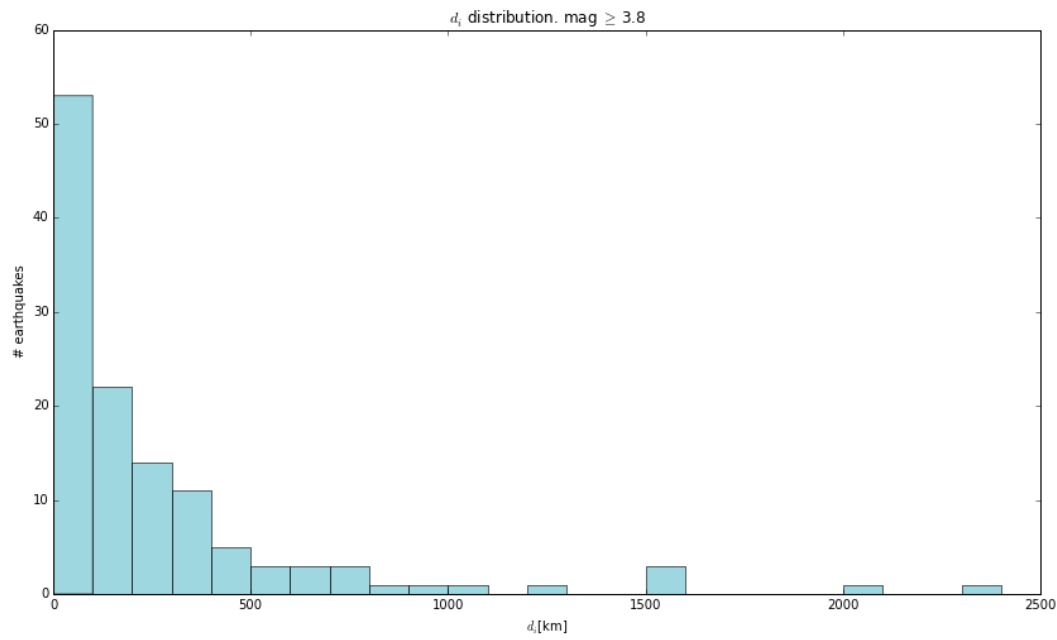


**Figure 9.** Local bandwidth example.



(a)



(b)

**Figure 10.** (a)  $h_i$  and (b)  $d_i$  distributions from BSB.

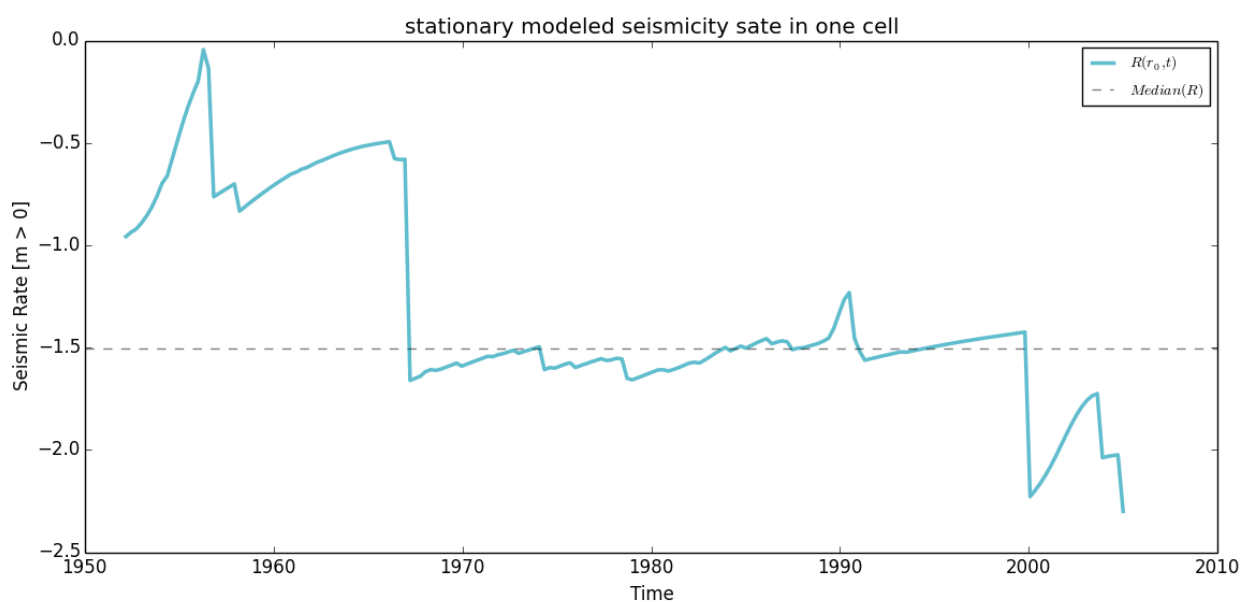


**Figure 11.** Stationary seismic rate

### BSB2014.11 learning and target catalogs

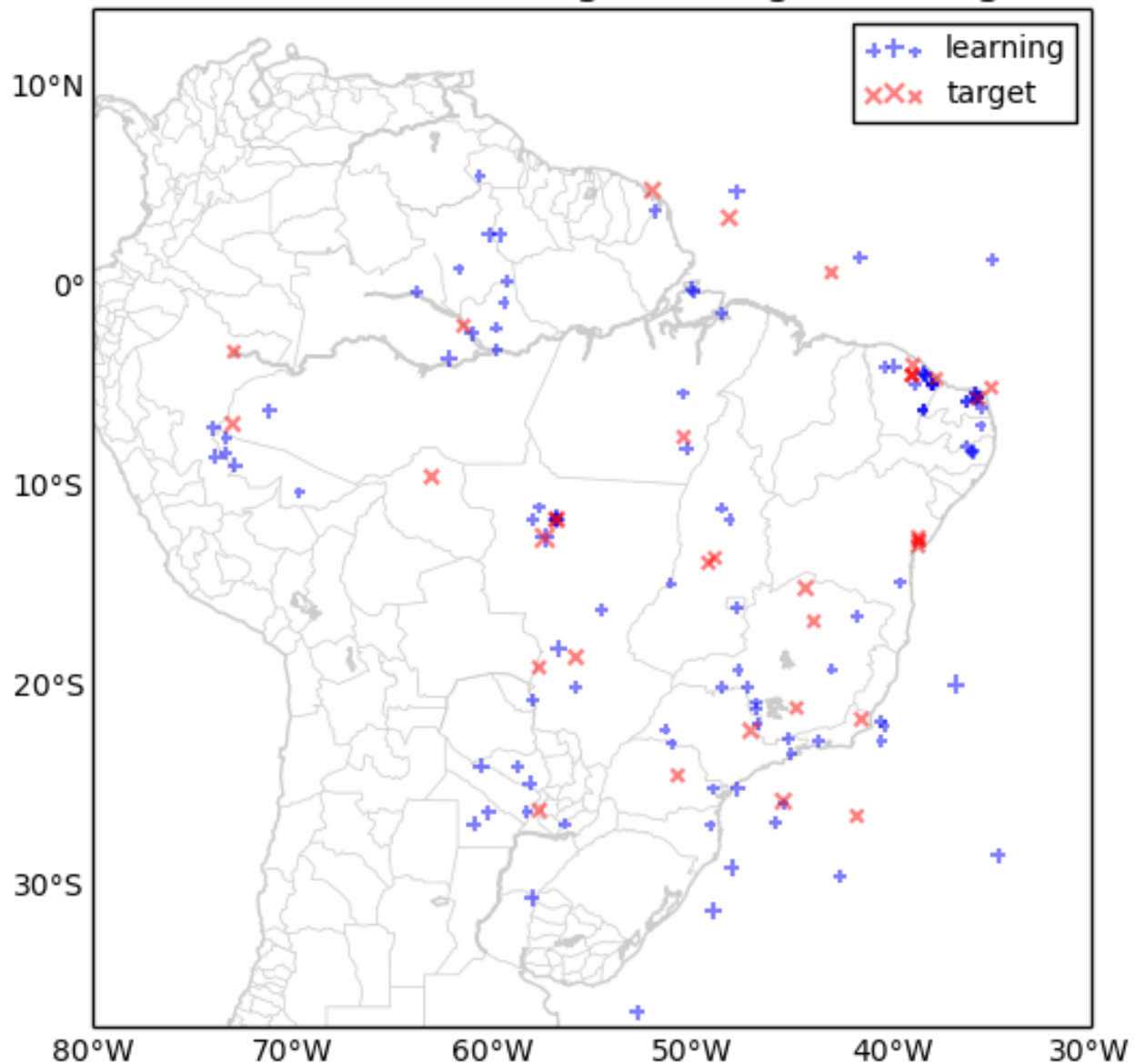


**Figure 12.** Learning and testing catalogs.

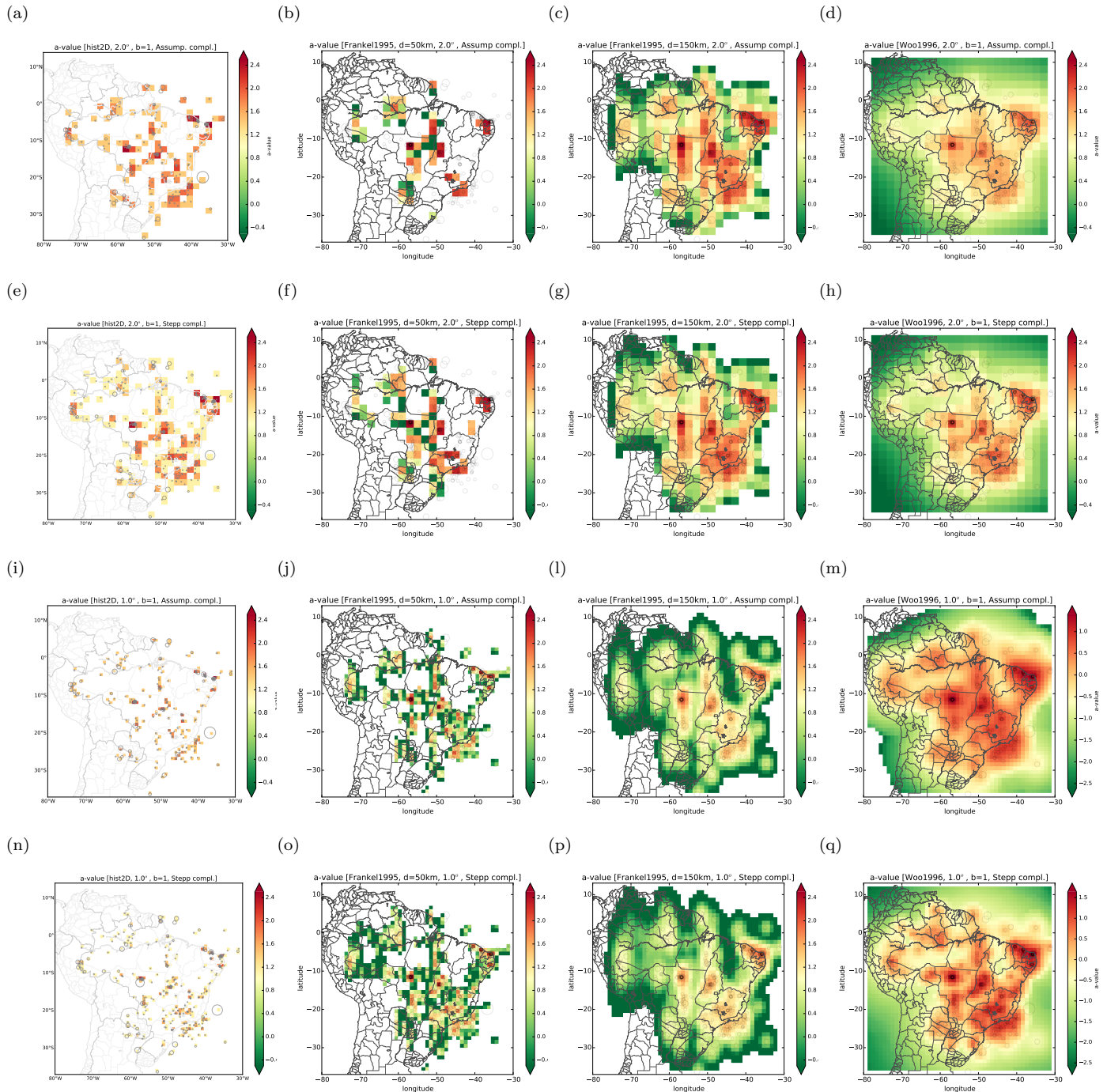


**Figure 13.** Smoothed rates comparission: (a) shows *Frankel* [1995] method smoothed rate results, (b) and (c) represent rates smoothed by *Woo* [1996] and *Helmstetter and Werner* [2012] methods respectively.

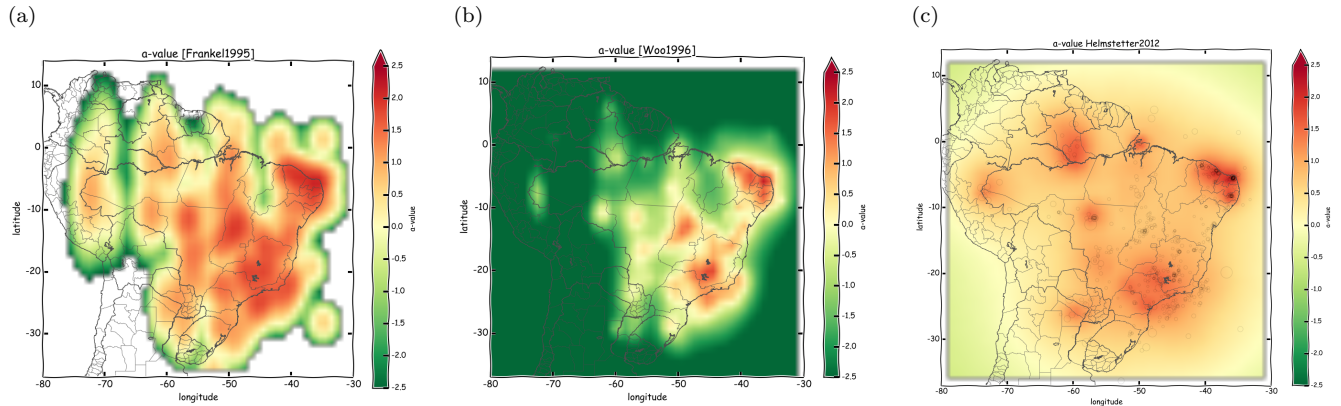


**Figure 14.** Smoothed rates comparission: (a) shows *Frankel* [1995] method smoothed rate results, (b) and (c) represent rates smoothed by *Woo* [1996] and *Helmstetter and Werner* [2012] methods respectively.

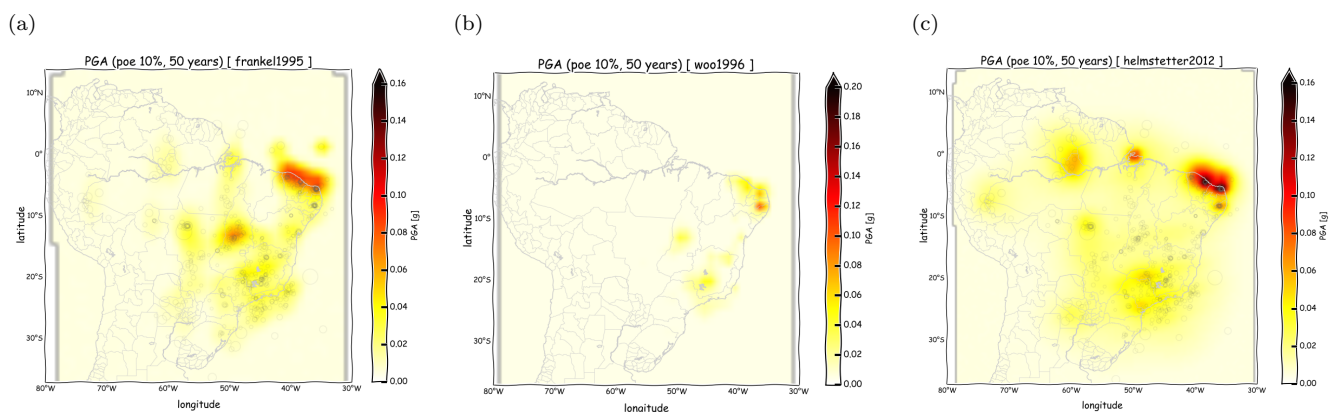


**Figure 15.** PGA (poe 10%/50y) comparission for (a) *Frankel* [1995], (b) *Woo* [1996] and (c) *Helmstetter and Werner* [2012] methods.

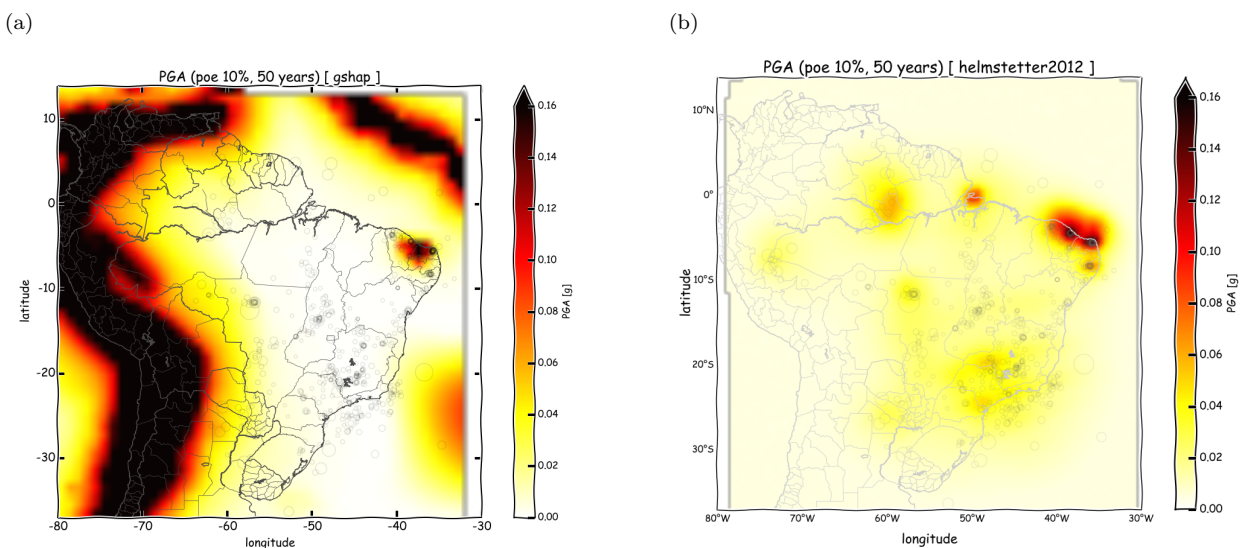


**Figure 16.** Previous available Brazilian PSHA from (a) GSHAP project and the PSHA proposed by this work (b).